

Active control of vibrations in pedestrian bridges

Álvaro Cunha & Carlos Moutinho

Faculty of Engineering of the University of Porto, Portugal

ABSTRACT: This paper, apart from making a brief general reference to vibration problems in pedestrian bridges, as well as to the form of modelling of dynamic pedestrian loads, presents the use of a predictive control strategy for the numerical simulation of the dynamic response of actively controlled structures of this type. The consideration of this control strategy permitted the development of a computational model, which was applied to the study of a pedestrian cable-stayed bridge, in order to show the interest and efficiency of the active control technique used.

1 VIBRATION PROBLEMS IN PEDESTRIAN BRIDGES

Pedestrian bridges tend to become more and more light and flexible structures, whose first natural frequencies of vibration may fall close to dominant frequencies of the dynamic excitation due to walking or running, leading to a resonant response characterised by high levels of vibration (Bachmann & Ammann 1987). Although such vibrations don't cause usually structural problems, they can induce some uncomfortable sensation, and so some codes or standards establish maximum acceptable values of vertical acceleration, normally expressed as function of the fundamental frequency of the bridge.

It is therefore interesting to develop numerical models that enable to appropriately simulate the dynamic response of pedestrian bridges under human loads when either a passive or an active control system is included to attenuate the high level of vibrations.

In this context, this paper makes a brief description of an investigation conducted with the aim of applying an active control technique to reduce vibrations in pedestrian bridges, presenting the details of the predictive control strategy used (previously developed and applied by Cascante *et al* 1993, in the context of Earthquake Engineering), which permitted the development of a computational model for the numerical simulation of the dynamic response of actively controlled pedestrian bridges. This program was applied to the study of a real pedestrian cable-stayed bridge, in order to show the interest and efficiency of this control technique.

2 DYNAMIC PEDESTRIAN LOADS

Three different types of human motion are commonly considered to model the dynamic loads applied by pedestrians (Bachmann *et al* 1987, 1995), namely walking, running and rhythmic jumping. The pacing rate ($f_p = 1/T_p$) and the pedestrian forward speed (v_p) are two parameters that play a fundamental role in terms of the characterisation of the excitation, the corresponding average values being presented in Table 1 for walking or running.

Table 1. Average values of f_p and v_p

Type of motion	Walking			Running	
	slow	normal	fast	slow	fast
f_p (Hz)	1.7	2.0	2.3	2.5	3.2
v_p (m/s)	1.1	1.5	2.2	3.3	>5.5

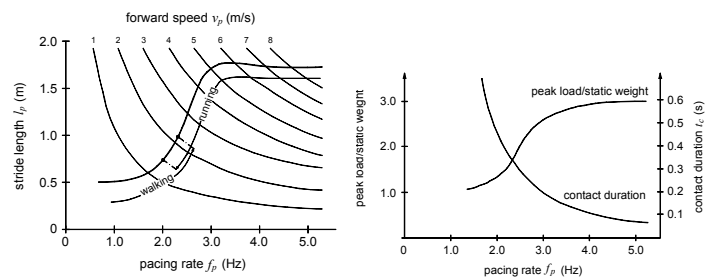


Figure 1. Experimental relations between load parameters

Other important quantities directly related with these two parameters are the stride length ($l_p = v_p / f_p$), the ground contact duration (t_c) and the load peak factor (F_a), relating the maximum applied load with

the pedestrian weight (G). Experimental relations obtained between these parameters are expressed in Figure 1.

The characterisation of the temporal evolution of the pedestrian loads can then be performed using appropriate load-time functions (Bachmann *et al* 1987, 1995), such as:

- Walking

$$F_p(t) = G + \sum_{i=1}^n G\alpha_i \sin(2\pi f_p t - \phi_i) \quad (1)$$

where

$$\alpha_1 = 0.43 f_p - 0.38, \alpha_2 = 0.15 f_p - 0.125 \geq 0.1, \\ \alpha_3 = 0.1, \phi_1 = 0 \text{ and } \phi_2 = \phi_3 = \pi/2;$$

- Running (semi-sinusoidal time-load function)

$$F_p(t) = \begin{cases} K_p G \sin(\pi t / t_c) & , t \leq t_c \\ 0 & , t_c < t \leq T_p \end{cases} \quad (2)$$

$$\text{where } K_p = \pi / 2 f_p t_c;$$

- Rhythmic jumping (triangular time-load function)

$$F_p(t) = \begin{cases} K_p G (2t / t_c) & , t \leq t_c / 2 \\ K_p G \left(1 - \frac{2(t - t_c / 2)}{t_c}\right) & , t_c / 2 < t \leq t_c \\ 0 & , t_c < t \leq T_p \end{cases} \quad (3)$$

$$\text{where } K_p = 2 / f_p t_c.$$

It's worth noting however that the periodicity of the input also allows alternative Fourier series representations.

3 ACTIVE CONTROL OF VIBRATIONS USING A PREDICTIVE STRATEGY

3.1 State-space formulation

The equation of motion of a MDOF linear system submitted to an external excitation $\underline{f}(t)$ and to a control load $\underline{f}_c(t)$ is

$$\underline{M}\ddot{\underline{d}}(t) + \underline{C}\dot{\underline{d}}(t) + \underline{K}\underline{d}(t) = \underline{f}_c(t) + \underline{f}(t) \quad (4)$$

where \underline{M} , \underline{C} , and \underline{K} are the mass, damping and stiffness matrices, and \underline{d} , $\dot{\underline{d}}$ and $\ddot{\underline{d}}$ are the vectors of displacements, velocities and accelerations in correspondence with the n degrees of freedom.

Introducing a state space representation, this equation can be transformed into $2n$ first order differential equations, expressed by

$$\dot{\underline{x}} = \underline{F}\underline{x} + \underline{v}_c + \underline{v} \quad (5)$$

where the state vector \underline{x} , the system matrix \underline{F} and the vectors \underline{v}_c and \underline{v} are given by

$$\underline{x} = \begin{bmatrix} \underline{d} \\ \dot{\underline{d}} \end{bmatrix} \quad \underline{F} = \begin{bmatrix} \underline{0} & \underline{I} \\ -\underline{M}^{-1}\underline{K} & -\underline{M}^{-1}\underline{C} \end{bmatrix} \\ \underline{v}_c = \begin{bmatrix} \underline{0} \\ \underline{M}^{-1}\underline{f}_c \end{bmatrix} \quad \underline{v} = \begin{bmatrix} \underline{0} \\ \underline{M}^{-1}\underline{f} \end{bmatrix} \quad (6)$$

The solution of equation (5), based on a discrete time model associated to a time resolution Δt , can be expressed by the relation

$$\underline{x}(k\Delta t + \Delta t) = e^{\Delta t \underline{F}} \underline{x}(k\Delta t) + \int_{k\Delta t}^{(k+1)\Delta t} e^{[(k+1)\Delta t - \tau] \underline{F}} [\underline{v}_c(\tau) + \underline{v}(\tau)] d\tau \quad (7)$$

where $k\Delta t$ means a generic time instant.

Assuming that the control forces are constant along the time interval $[k\Delta t, (k+1)\Delta t]$, and that the external load varies linearly in that same interval, equation (7) can be written in the following form, introducing the variable $\mu = (k+1)\Delta t - \tau$

$$\underline{x}(k\Delta t + \Delta t) = e^{\Delta t \underline{F}} \underline{x}(k\Delta t) + \\ + \int_0^{\Delta t} e^{\mu \underline{F}} \left[(\Delta t - \mu) \frac{\underline{v}(k\Delta t + \Delta t) - \underline{v}(k\Delta t)}{\Delta t} + \underline{v}(k\Delta t) \right] d\mu + \\ + \int_0^{\Delta t} e^{\mu \underline{F}} \underline{v}_c(k\Delta t) d\mu \quad (8)$$

This equation can still be expressed in the simpler compact matricial form, omitting the time interval Δt

$$\underline{x}(k+1) = \underline{A}\underline{x}(k) + \underline{P}_1 \underline{v}(k+1) + \underline{P}_2 [\underline{v}(k+1) - \underline{v}(k)] + \underline{P}_1 \underline{v}_c(k) \quad (9)$$

where \underline{A} (time discrete system matrix), \underline{P}_1 and \underline{P}_2 are the following $(2n \times 2n)$ matrices

$$\underline{A} = e^{\Delta t \underline{F}} \quad \underline{P}_1 = \underline{F}^{-1}(\underline{A} - \underline{I}) \quad \underline{P}_2 = \underline{F}^{-1} \left(\frac{1}{\Delta t} \underline{P}_1 - \underline{A} \right) \quad (10)$$

Once $\underline{x}(k+1)$ is known, the vector of accelerations can be obtained using the following numerical procedure

$$\ddot{d}(k+1) = \frac{\dot{d}(k+1) - \dot{d}(k)}{\Delta t} \quad (11)$$

3.2 Predictive model

The dynamic response of a MDOF linear system submitted to an external excitation and to a control load can be represented by the following first order discrete model, using a state space formulation (Cascante *et al* 1993)

$$\underline{x}(k+1) = \underline{A}\underline{x}(k) + \underline{B}\underline{u}(k - n_r) + \underline{w}(k) \quad (12)$$

where \underline{A} is the time discrete system matrix and \underline{B} is the time discrete control matrix. $\underline{x}(k)$ is the state vector at the instant k and $\underline{w}(k)$ is the vector that represents the excitation. $\underline{u}(k - n_r)$ is the control vector generated at the instant $k - n_r$, where n_r characterises the time delay of the actuators.

The following equivalence can be then established between equations (9) and (12)

$$\underline{w}(k) = \underline{P}_1 \underline{v}(k+1) + \underline{P}_2 [\underline{v}(k+1) - \underline{v}(k)] \quad (13)$$

$$\underline{P}_1 \underline{v}_c(k) = \underline{B}\underline{u}(k - n_r) \quad (14)$$

As $\underline{u}(k - n_r)$ is a vector with a number of components equal to the number of actuators, n_a , and $\underline{v}_c(k)$ is the vector with $2n$ components defined by equation (6), one can write

$$\underline{v}_c(k) = \begin{bmatrix} \underline{0} \\ \underline{M}^{-1} \underline{J} \end{bmatrix} \underline{u}(k - n_r) = \underline{L}\underline{u}(k - n_r) \quad (15)$$

where \underline{J} is a matrix $(n \times n_a)$, whose elements are equal to 1 or 0, depending on the presence of actuators in correspondence with the n degrees of freedom. Therefore

$$\underline{B} = \underline{P}_1 \underline{L} = \underline{P}_1 \begin{bmatrix} \underline{0} \\ \underline{M}^{-1} \underline{J} \end{bmatrix} \quad (16)$$

The structural response, expressed in terms of other control variables, $\underline{y}(k)$, can be obtained on the basis of the state vector $\underline{x}(k)$ using a linear transformation

$$\underline{y}(k) = \underline{H}\underline{x}(k) \quad (17)$$

where \underline{H} is called output matrix.

The prediction of the temporal evolution of the structural response along the interval of time $[k, k + \lambda + \hat{n}_r]$, where λ is a horizon of prediction and

\hat{n}_r is the estimate number of periods of time delay of the actuators, can be performed on the basis of the following model, disregarding the contribute of the excitation after the time instant k (*simplified prediction model*)

$$\begin{aligned} \hat{\underline{x}}(k+j|k) &= \hat{\underline{A}}\hat{\underline{x}}(k+j-1|k) + \hat{\underline{B}}\hat{\underline{u}}(k+j-1-\hat{n}_r|k) \\ \hat{\underline{y}}(k+j|k) &= \hat{\underline{H}}\hat{\underline{x}}(k+j|k) \end{aligned} \quad (18,19)$$

where the vectors $\hat{\underline{x}}(k+j|k)$ and $\hat{\underline{y}}(k+j|k)$ ($j=1, \dots, \lambda + \hat{n}_r$) are, respectively, the state vector and the output vector at the instant $k+j$, predicted at the instant k , and $\hat{\underline{u}}(k+j-1-\hat{n}_r|k)$ is the control vector at the instant $k+j-1-\hat{n}_r$, predicted at the instant k . Note that the symbol ($\hat{\cdot}$) always means an estimate.

The sequence of control vectors $\hat{\underline{u}}(k|k), \dots, \hat{\underline{u}}(k+\lambda-1|k)$ can be evaluated using a criterion based on the minimisation of the following cost function (Cascante *et al* 1993)

$$\begin{aligned} J &= \frac{1}{2} \sum_{j=1}^{\lambda+\hat{n}_r} [\hat{\underline{y}}(k+j|k) - \underline{y}_r(k+j|k)]^T \cdot \\ &\cdot \underline{Q}_j [\hat{\underline{y}}(k+j|k) - \underline{y}_r(k+j|k)] + \\ &+ \frac{1}{2} \sum_{j=0}^{\lambda-1} \hat{\underline{u}}(k+j|k)^T \underline{R}_j \hat{\underline{u}}(k+j|k) \end{aligned} \quad (20)$$

where $\underline{y}_r(\cdot|k)$ means a sequence of output vectors that characterises the desired trajectory of the system, starting from its real position at the instant k . \underline{Q}_j ($j=1, \dots, \lambda + \hat{n}_r$) and \underline{R}_j ($j=0, \dots, \lambda-1$) are symmetric weighting matrices.

In order to reduce the number of variables in this optimisation problem, two different simplifications can be considered:

- (i) To assume that the strategy of control is just based on the minimisation of the difference between the predicted response $\hat{\underline{y}}$ and the reference trajectory \underline{y}_r at the horizon of prediction $k + \lambda + \hat{n}_r$, which implies

$$\underline{Q}_1 = \dots = \underline{Q}_{\lambda+\hat{n}_r-1} = \underline{0} \quad \underline{Q}_{\lambda+\hat{n}_r} = \underline{Q} \quad (21)$$

- (ii) To consider a sequence of constant vectors of control $\hat{\underline{u}}(\cdot|k)$ in the time interval $[k, k + \lambda - 1]$

$$\underline{u}(k) = \hat{\underline{u}}(k|k) = \hat{\underline{u}}(k+1|k) = \dots = \hat{\underline{u}}(k+\lambda-1|k) \quad (22)$$

Introducing these simplifications, equation (20) takes simply the form

$$J = \frac{1}{2} \left[\hat{y}(k + \lambda + \hat{n}_r | k) - \underline{y}_r(k + \lambda + \hat{n}_r | k) \right]^T \cdot \underline{Q} \left[\hat{y}(k + \lambda + \hat{n}_r | k) - \underline{y}_r(k + \lambda + \hat{n}_r | k) \right] + \frac{1}{2} \underline{u}(k)^T \underline{R} \underline{u}(k) \quad (23)$$

where $\underline{R} = \sum_{j=0}^{\lambda-1} \underline{R}_j$.

The matrices \underline{Q} and \underline{R} weight the influence of the difference between the predicted and reference responses and of the control signal, respectively, in the minimisation of J . Higher coefficients of \underline{Q} and lower coefficients of \underline{R} diminish the differences between \hat{y} and \underline{y}_r , but involve a more energetic control action. Higher coefficients of \underline{R} constrain the control signal, preventing a very efficient control action.

An expression for the vector $\hat{x}(k + \lambda + \hat{n}_r | k)$ can be obtained applying equation (18) repeatedly, which leads to

$$\begin{aligned} \hat{x}(k + \lambda + \hat{n}_r | k) &= \hat{A} \hat{x}(k + \lambda + \hat{n}_r - 1 | k) + \hat{B} \underline{u}(k) = \\ &= \hat{A}^{\hat{n}_r + \lambda} \underline{x}(k) + \hat{A}^{\hat{n}_r + \lambda - 1} \hat{B} \underline{u}(k - \hat{n}_r) + \dots + \\ &+ \hat{A}^{\lambda} \hat{B} \underline{u}(k - 1) + \hat{A}^{\lambda - 1} \hat{B} \underline{u}(k) + \\ &\hat{A}^{\lambda - 2} \hat{B} \underline{u}(k) + \dots + \hat{A} \hat{B} \underline{u}(k) + \hat{B} \underline{u}(k) \end{aligned} \quad (24)$$

or in a more compact form

$$\hat{x}(k + \lambda + \hat{n}_r | k) = \hat{T} \underline{x}(k) + \underline{\varphi}(k) + \hat{Z}_0 \underline{u}(k) \quad (25)$$

where

$$\hat{T} = \hat{A}^{\lambda + \hat{n}_r} \quad \underline{\varphi}(k) = \hat{Z}_1 \underline{u}(k - 1) + \dots + \hat{Z}_{\hat{n}_r} \underline{u}(k - \hat{n}_r)$$

$$\hat{Z}_i = \hat{A}^{\lambda + i - 1} \hat{B} \quad (i = 1, \dots, \hat{n}_r)$$

$$\hat{Z}_0 = (\hat{A}^{\lambda - 1} + \hat{A}^{\lambda - 2} + \dots + \hat{A}^2 + \hat{A} + I) \hat{B} \quad (26)$$

The corresponding output vector can then be expressed as (see eq. (17))

$$\hat{y}(k + \lambda + \hat{n}_r | k) = \hat{H} \hat{T} \underline{x}(k) + \hat{H} \underline{\varphi}(k) + \hat{H} \hat{Z}_0 \underline{u}(k) \quad (27)$$

The evaluation of the control vector involves the minimisation of the cost function J , which implies that

$$\frac{\partial J}{\partial \underline{u}(k)} = 0 \quad (28)$$

Taking into account that

$$\begin{aligned} \frac{\partial J}{\partial \underline{u}(k)} &= (\hat{H} \hat{Z}_0)^T \underline{Q} \cdot \\ &\cdot \left[\hat{H} \hat{T} \underline{x}(k) + \hat{H} \underline{\varphi}(k) + \hat{H} \hat{Z}_0 \underline{u}(k) - \underline{y}_r(k + \lambda + \hat{n}_r | k) \right] + \\ &+ \underline{R} \underline{u}(k) \end{aligned} \quad (29)$$

and that

$$\frac{\partial^2 J}{\partial^2 \underline{u}(k)} = (\hat{H} \hat{Z}_0)^T \underline{Q} (\hat{H} \hat{Z}_0) + \underline{R} \quad (30)$$

it is possible to conclude that the vector $\underline{u}(k)$ that minimises J is given by

$$\begin{aligned} \underline{u}(k) &= - \left[(\hat{H} \hat{Z}_0)^T \underline{Q} (\hat{H} \hat{Z}_0) + \underline{R} \right]^{-1} \cdot \\ &\cdot \left\{ (\hat{H} \hat{Z}_0)^T \underline{Q} \left[\hat{H} \hat{T} \underline{x}(k) + \hat{H} \underline{\varphi}(k) - \underline{y}_r(k + \lambda + \hat{n}_r | k) \right] \right\} \end{aligned} \quad (31)$$

Once the control vector is obtained, the analysis can proceed to the next time instant $k+1$, following the same predictive control strategy. It's worth noting that the evaluation of $\underline{u}(k)$ involves the inversion of the so-called Hessian matrix $(\hat{H} \hat{Z}_0)^T \underline{Q} (\hat{H} \hat{Z}_0) + \underline{R}$, and so matrices \underline{Q} and \underline{R} must be defined so that the Hessian matrix is definite positive.

4 SIMULATION OF ACTIVE CONTROL OF A CABLE-STAYED PEDESTRIAN BRIDGE

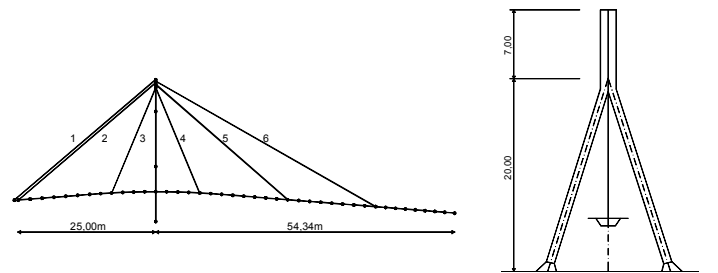


Figure 2. Schematic representation of the cable-stayed pedestrian bridge

The predictive control strategy previously described was applied to the numerical simulation of the controlled dynamic response of a pedestrian cable-stayed bridge (Figure 2) with the characteristics of a bridge existing at Martorell, near Barcelona, referred in (Cobo *et al* 1995).

Table 2. Characteristics of the bridge

Element	Area (m ²)	Inertia (m ⁴)	Tension (kN)	Mass (kg/m)
Deck	0.14	0.011	--	1950
Tower - legs	0.11	0.016	--	850
Tower - top	0.08	0.013	--	600
Stay cable 1	0.00442	--	675	46
Stay cable 2	0.00442	--	675	46
Stay cable 3	0.00196	--	305	34
Stay cable 4	0.00196	--	244	34
Stay cable 5	0.00442	--	526	53
Stay cable 6	0.00442	--	854	53

The evaluation of the most relevant modal characteristics of the bridge was based on the development of a 2D finite element model, in which the deck and tower were discretised in a set of beam elements, according to the schematic representation presented in Figure 2, whereas the behaviour of the stay cables was idealised using truss elements with an equivalent Young Modulus, to take into account the sag effect. The values of the first 4 natural frequencies, evaluated by a linear dynamic analysis performed using the stiffness matrix obtained at the end of a previous static analysis under permanent loads, considering the geometrical non-linearities, were: $f_1 = 1.705\text{Hz}$, $f_2 = 3.246\text{Hz}$, $f_3 = 3.835\text{Hz}$ and $f_4 = 5.649\text{Hz}$. The corresponding modal shapes are represented in Figure 3. The modal damping coefficients were assumed as 1%.

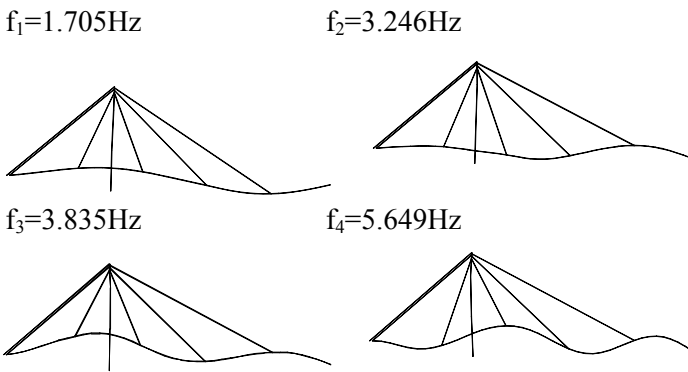


Figure 3. Calculated mode shapes

The values of natural frequencies obtained suggest that structural resonance due to pedestrian motions may occur, and so the following situations were particularly studied (Moutinho 1998): (i) walking with $f_p = f_1$; (ii) running with $f_p = f_2$ or $f_p = f_3$; (iii) jumping at the section of maximum amplitude of the second mode, with $f_p = f_2$. The analysis of the structural response was performed in those three cases, assuming the values of the several parameters involved in the time-load functions (eq. 1-3) referred in Tables 3-5, and applying the Newmark method.

Table 3. Parameters used in the load modelling (walking)

G (N)	f_p (Hz)	l_p (m)	α_1	α_2	α_3
700	1.705	0.60	0.353	0.131	0.100
			ϕ_1	ϕ_2	ϕ_3
			0	$\pi/2$	$\pi/2$

Table 4. Parameters used in the load modelling (running)

G (N)	f_p (Hz)	T_p (s)	t_c (s)	K_p	l_p (m)
700	3.246	0.308	0.15	3.226	1.75
700	3.835	0.261	0.11	3.724	1.75

Table 5. Parameters used in the load modelling (jumping)

G (N)	f_p (Hz)	T_p (s)	t_c (s)	K_p
700	3.246	0.308	0.15	4.108

The corresponding peak values calculated in terms of vertical displacements, velocities and accelerations at three control sections A, B and C (sections of maximum amplitude of the first three mode shapes, respectively) are summarised in Table 6.

Table 6. Peak values of the response without control

Action	Peak values		
	Displ. (m)	Veloc. (m/s)	Accel.(m/s ²)
Walking ($f_p=f_1$)	0.00119	0.0115	0.124
Running ($f_p=f_2$)	0.00145	0.0288	0.609
Running ($f_p=f_3$)	0.00109	0.0254	0.712
Jumping ($f_p=f_2$)	0.00249	0.0499	1.054

Considering, for instance, the maximum limit of vibration referred in the canadian standard ONT 83 (Bachmann *et al* 1995), defined by the expression $a_{\max} \leq 0.25 f_1^{0.78}$, the maximum vertical acceleration of 0.379m/s^2 is not exceeded only in the first situation (walking).

Therefore, it was assumed the introduction of an active control system, based on the use of a force actuator placed at an intermediate section of the deck between the anchorage points of the stay cables 4 and 5 (at a distance of 41.65m from the left extremity), so as to easily control the first three modal contributes, the structural response being measured by three sensors located at the sections of maximum amplitude of those modes of vibration.

The numerical simulation of the dynamic response of the actively controlled structure was performed applying the predictive control strategy described, considering $\Delta t=0.01\text{s}$, $\lambda=3$, $n_r=0$ and a null reference structural response. The weighting matrix \underline{Q} was assumed as

$$\underline{Q} = \begin{bmatrix} \underline{I} & \underline{0} \\ \underline{0} & \underline{0} \end{bmatrix} \quad (32)$$

whereas the matrix \underline{R} , that takes the form of a simple scalar R in this case, was iteratively adjusted in order to obtain a maximum vertical acceleration inferior to the maximum limit adopted for any of the several actions considered. The maximum accelerations calculated with and without the inclusion of the control system, as well as the maximum values of the control forces are summarised in Table 7. The temporal evolution of the structural response at section C due to the passage of a pedestrian running with $f_p=f_3$ is illustrated in Figure 4, the evolution of the corresponding control force being represented in Figure 5.

Table 7. Peak values of acceleration and control force

Action	Maximum accel. (m/s ²)		Reduction (%)	Max. control force (N)
	without control	with control		
Walking ($f_p=f_1$)	0.124	0.035	72	578
Running ($f_p=f_2$)	0.609	0.178	70	1272
Running ($f_p=f_3$)	0.695	0.368	47	1372
Jumping ($f_p=f_2$)	1.054	0.217	80	1482

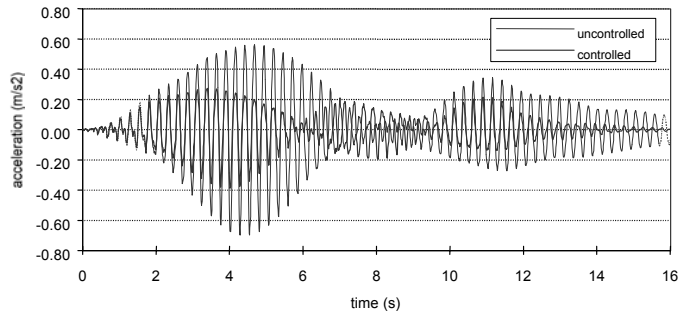


Figure 4. Vertical accelerations at section C (running, $f_p=f_3$)

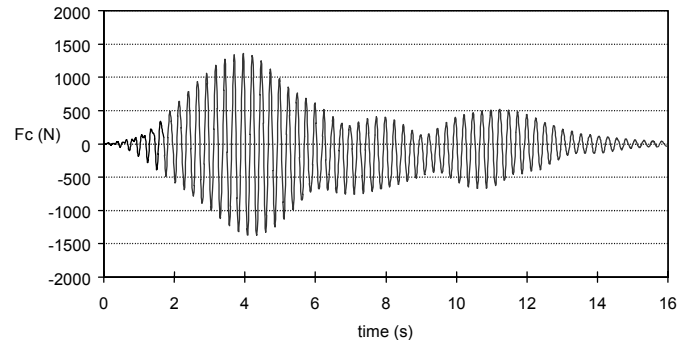


Figure 5. Control force (running, $f_p=f_3$)

5 CONCLUSIONS

Human beings, when walking, running or jumping on structures can apply dynamic loads that can be responsible by excessive levels of vibration, which can be attenuated both using passive and active control techniques. In this last case, the instantaneous definition of an appropriate value of one or more control forces involves the use of a suitable control strategy. Among several alternative control strategies, the predictive control technique used in this work seems to be rather general, versatile and fairly easily implemented. Moreover, the significant reduction of levels of vibration achieved in the numerical simulations presented evidence the good efficiency attained. Therefore the authors intend to give now a new step forward in the present investigation, making a real implementation of this active control technique, conjugating the present control strategy with the use of an active mass damper in a pedestrian bridge.

AKNOWLEDGEMENTS

The authors aknowledge the elements provided by Prof. Rodellar and Prof. Diego Cobo, from UPC (Barcelona), as well as the support given by the Portuguese Foundation for Science and Technology (FCT) in the context of the Research Project nº PBIC/CEG/2349/95.

REFERENCES

Bachmann, H. & Ammann, W. 1987. *Vibrations in structures induced by men and machines*, Zürich: IABSE.

Bachmann, H. *et al.* 1995. *Vibration problems in structures. Practical guidelines*, Basel: Birkhäuser Verlag.

Cascante, R.A., Rodellar, J. & Almansa, F.L. 1993. *Control predictivo en sistemas de protección sísmica de estructuras*, Barcelona: CIMNE.

Cobo, D., Vilarrasa, J.C. & Bernat, A.M. 1995. Dynamic analysis of a cable-stayed pedestrian bridge – a case study. In Proc. Int. Symposium on Cable Dynamics, Liege, pp.101-108.

Moutinho, C. 1998. *Passive and active control of vibrations in pedestrian bridges*, M.Sc. Thesis (in Portuguese), Faculty of Engineering of the University of Porto (FEUP), Portugal.